


# Role of calcium integrin-binding protein 1 in the mechanobiology of the liver endothelium

Cong Wang<sup>1</sup> | Eric Felli<sup>1,2</sup> | Sonia Selicean<sup>1</sup> | Yelidusi Nulan<sup>1</sup> | Juan José Lozano<sup>3</sup> | Sergi Guixé-Muntet<sup>3</sup> | Jaume Bosch<sup>1,2,3</sup> | Annalisa Berzigotti<sup>1,2</sup> | Jordi Gracia-Sancho<sup>1,2,3</sup> 

<sup>1</sup>Department of Visceral Surgery and Medicine, Inselspital, Bern University Hospital, University of Bern, Bern, Switzerland

<sup>2</sup>Department for BioMedical Research, Visceral Surgery and Medicine, University of Bern, Bern, Switzerland

<sup>3</sup>Liver Vascular Biology Research Group, IDIBAPS Biomedical Research Institute, CIBEREHD, Barcelona, Spain

**Correspondence** Jordi Gracia-Sancho, Inselspital, Bern University Hospital, Murtenstrasse 35, 8003, Bern, Switzerland. Email: [jordi.gracia@unibe.ch](mailto:jordi.gracia@unibe.ch) and [jgracia@recerca.clinic.cat](mailto:jgracia@recerca.clinic.cat)

## Funding information

Schweizerischer Nationalfonds zur Förderung der Wissenschaftlichen Forschung; Swiss National Science Foundation, Grant/Award Number: SNF 320030\_189252/1; Novartis Foundation; Swiss Foundation Against Liver Cancer; Instituto de Salud Carlos III, Grant/Award Numbers: FIS PI20/00220, PI23/00945, DTS22/00010; European Union; AGAUR-Generalitat de Catalunya, Grant/Award Numbers: 2021 SGR 01322, 2021 PROD 00036; China Scholarship Council; Stiftung für Leberkrankheiten; Juan Rodés Fellowship from the European Association for the Study of the Liver; Department of Visceral Surgery and Medicine, Inselspital; Swiss Government Excellence Scholarships; Sara Borrell Fellowship from Instituto de Salud Carlos III

## Abstract

Liver sinusoidal endothelial cells (LSECs) dysfunction is a key process in the development of chronic liver disease (CLD). Progressive scarring increases liver stiffness in a winch-like loop stimulating a dysfunctional liver cell phenotype. Cellular stretching is supported by biomechanically modulated molecular factors (BMMFs) that can translocate into the cytoplasm to support mechanotransduction through cytoskeleton remodeling and gene transcription. Currently, the molecular mechanisms of stiffness-induced LSECs dysfunction remain largely unclear. Here we propose calcium- and integrin-binding protein 1 (CIB1) as BMMF with crucial role in LSECs mechanobiology in CLD. CIB1 expression and translocation was characterized in healthy and cirrhotic human livers and in LSECs cultured on polyacrylamide gels with healthy and cirrhotic-like stiffnesses. Following the modulation of CIB1 with siRNA, the transcriptome was scrutinized to understand downstream effects of CIB1 downregulation. CIB1 expression is increased in LSECs in human cirrhosis. In vitro, CIB1 emerges as an endothelial BMMF. In human umbilical vein endothelial cells and LSECs, CIB1 expression and localization are modulated by stiffness-induced trafficking across the nuclear membrane. LSECs from cirrhotic liver tissue both in animal model and human disease exhibit an increased amount of CIB1 in cytoplasm. Knockdown of CIB1 in LSECs exposed to high stiffness improves LSECs phenotype by regulating the intracellular tension as well as the inflammatory response. Our results demonstrate that CIB1 is a key factor in sustaining cellular tension and stretching in response to high stiffness. CIB1 downregulation ameliorates LSECs dysfunction, enhancing their redifferentiation, and reducing the inflammatory response.

**Abbreviations:** BMMFs, biomechanically modulated molecular factors; BSA, bovine serum albumin; Ca<sup>2+</sup>, calcium; CCL22, C-C motif chemokine 22; CCR4, CC chemokine receptor 4; CD, cytoskeleton disruption; CIB1, calcium- and integrin-binding protein 1; CLD, chronic liver disease; CT, negative control; DAPI, 4',6-diamidino-2-phenylindole; DEGs, differentially expressed genes; DMSO, dimethyl sulfoxide; ECGS, endothelial cell growth supplement; ECM, extracellular matrix; FC, fold change; GEO, gene expression omnibus; GOBP, gene ontology biological process; GOCC, gene ontology cellular component; GSEA, gene set enrichment analysis; HUVECs, human umbilical vein endothelial cells; ITG β-1, integrin beta 1; KEGG, kyoto encyclopedia of genes and genomes; LSECs, liver sinusoidal endothelial cells; NES, normalized enrichment score; PAA, polyacrylamide gels; PH, portal hypertension; siRNA, small interfering RNA; SRA, sequence read archive; TAA, thioacetamide; αSMA, alpha smooth muscle actin.

Cong Wang, Eric Felli, and Sonia Selicean contributed equally to this work.

This is an open access article under the terms of the [Creative Commons Attribution-NonCommercial](https://creativecommons.org/licenses/by-nc/4.0/) License, which permits use, distribution and reproduction in any medium, provided the original work is properly cited and is not used for commercial purposes.

© 2024 The Authors. *Journal of Cellular Physiology* published by Wiley Periodicals LLC.

## KEYWORDS

chronic liver disease, liver sinusoidal endothelial cells, mechanotransduction, stiffness

## 1 | INTRODUCTION

Liver fibrosis in chronic liver disease (CLD) is a major driver of the progression to end stage liver failure and portal hypertension (PH). Among the pathophysiological mechanisms driving the development of fibrosis and PH, the dysfunction of liver sinusoidal endothelial cells (LSECs) is an early event, and plays a major role (Gracia-Sancho et al., 2019, 2021). Liver fibrosis is characterized by an increased stiffness as compared to healthy liver tissue, and measurement of stiffness is used routinely in hepatology. This physical property of liver tissue has proven to predict accurately the presence of PH (Berzigotti, 2017; Berzigotti et al., 2013) and liver-related mortality (Trebicka et al., 2022). Previous studies from our group and others have shown that stiffness of the environment modulates liver cells phenotype by altering the nuclear morphology through cytoskeleton-derived mechanical forces, thus modifying the nuclear permeability of biomechanically-modified molecular factors (BMMFs) (Andreu et al., 2022; Kalukula et al., 2022). Adhesion molecules such as integrins (Fletcher & Mullins, 2010) support cell-extracellular matrix (ECM) interactions, physically linking the ECM to the cytoskeleton and intracellular signaling apparatus (Kanchanawong & Calderwood, 2022; Slack et al., 2022) in a calcium ( $\text{Ca}^{2+}$ )-dependent manner (Miroshnikova et al., 2021).

Recent studies have shown how liver stiffness per se induces LSECs dedifferentiation and dysfunction (Guixé-Muntet et al., 2020) as well as alters angiocrine signaling inducing a proinflammatory phenotype (Greuter et al., 2022). However, the role of BMMFs in the molecular mechanisms underlying stiffness-mediated LSECs dysfunction remains largely unknown. Calcium- and integrin-binding protein 1 (CIB1) is a ubiquitous protein that is involved in mechanobiology by regulating integrin activation (Freeman et al., 2013), microtubule organization (Freeman et al., 2013; Naik & Naik, 2011), and vascular remodeling (Armacki et al., 2014; Grund et al., 2019; Zayed et al., 2007, 2010). Indeed, CIB1 can directly interact with and regulate focal adhesions via PAK1 (Leisner et al., 2005), affecting actin assembly during cell mechanotransduction (Martin et al., 2016). Increased intracellular  $\text{Ca}^{2+}$  due to cellular stretching (Rosales et al., 1997) stabilizes CIB1 structure and modulates its activity. This facilitates its interaction with other proteins related to mechanosensing (Leisner et al., 2016) and allows it to exert different functions as a transporter and modulator. Interestingly, given its low molecular weight (21 kDa), CIB1 may be able to passively translocate between the nucleus and the cytoplasm upon nuclear stretching. This suggests that CIB1 may accumulate in a  $\text{Ca}^{2+}$ -dependent manner in the cytoplasm and consequently modify cell phenotype. This study is aimed at elucidating the role of CIB1 in the mechanobiology of stiffness-induced dysfunction of LSECs in CLD.

## 2 | RESULTS

## 2.1 | CIB1 is involved in the cellular response to stress and upregulated in human cirrhotic LSECs

We used Enrichr ARCHS4 RNA-seq gene-gene coexpression matrix to improve the current understanding of CIB1 by identifying the top 200 coexpressed genes (Supporting Information S1: Table 1). Analysis of Reactome with Enrichr-KG of the pre-expanded gene list suggests that CIB1 may be involved in mechanoresponse-related effects, such as cellular response to stress and inflammation (Figure 1a). Functional classification of pathways showed that the inflammation mediated by chemokines and cytokine signaling pathway (P00031) was the most strongly involved (Figure 1b). Additionally, mechanobiology-related pathways were also represented, including the integrin signaling pathway (P00034) and cytoskeletal regulation by Rho GTPase (P00016). We further investigated the status of CIB1 in CLD using a human transcriptomic data set published by our group (GSE164799), showing that CIB1 was upregulated in cirrhotic patients (fold change cirrhotic/non-cirrhotic = 2.469;  $p = 0.007$ ). Immunostaining conducted in an internal cohort of patients (Supporting Information S1: Table 2) confirmed that CIB1 was upregulated in LSECs of cirrhotic livers (Figure 1c and Supporting Information S1: Figure 1), providing a preliminary insight into the involvement of CIB1 in CLD.

## 2.2 | Stiffness modulates CIB1 expression in human endothelial cells

To understand the sole effect of stiffness on CIB1 expression in human endothelial cells, we planned further in vitro experiments. Human umbilical vein endothelial cells (HUVECs) were cultured at healthy (0.5 kPa) and cirrhotic-like (30 kPa) stiffness and due to possible stiffness-induced epigenetic modifications acquired during cell expansion (in plastic support ~GPa) (Killaars et al., 2019; Nasrollahi et al., 2017; Walker et al., 2021), we found the optimal timepoint for nuclear and cell stretching by culturing cells for 2, 24, and 72 h. As shown in Figure 2a, nuclear area was significantly increased at 72 h. Similarly, cellular stretching and cell adhesion analyzed by ITGB1 (Cooper & Giancotti, 2019) expression showed a significant increase at 72 h (Figure 2b). We evaluated effective nuclear deformation via Lamin A staining, which confirmed 72 h as the optimal timepoint (Figure 2c,d). We further characterized the cell tension at high stiffness via  $\alpha$ SMA immunostaining (Figure 2e). Immediately after cell attachment, intracellular  $\text{Ca}^{2+}$  increases, while signaling pathways are activated within minutes (mechanosensing), such as the RhoA GTPase (Parsons et al., 2010). On the contrary, gene expression and epigenetic changes require hours or days to adapt to a different stiffness. Therefore, we

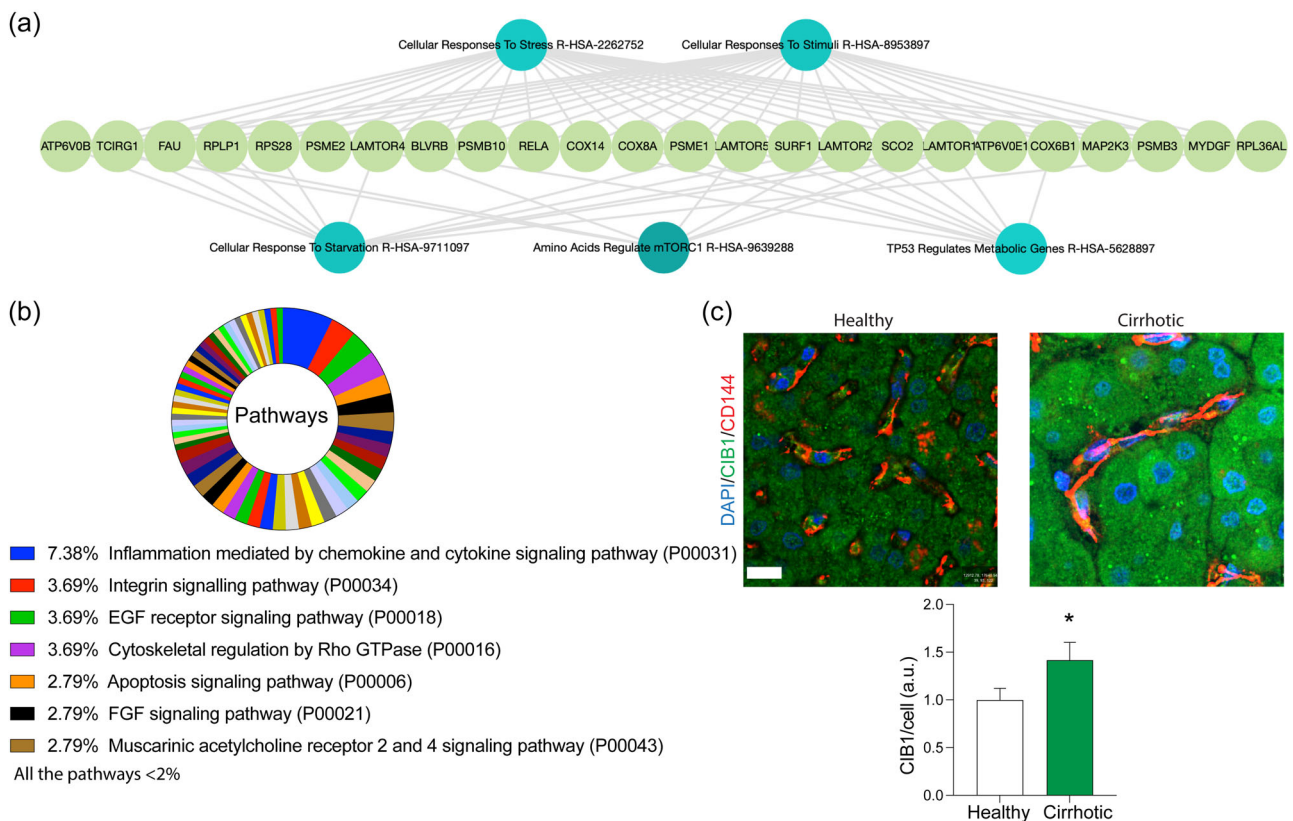


**FIGURE 1** CIB1 is involved in cellular stress and inflammation and overexpressed in liver cirrhosis. (a) CIB1 pre-expansion with Enrichr or Reactome hierarchical layout. (b) Gene lists extracted with Enricher were further analyzed to observe functional classification of pathways with Panther. (c) Immunofluorescence of endothelial CIB1 in human tissue ( $n = 10$  healthy,  $n = 10$  cirrhotic). Overall, 200 cells were analyzed in healthy and cirrhotic patients. All scale bars = 20  $\mu\text{m}$ . Data are expressed as mean  $\pm$  SEM. Normally distributed data were compared with unpaired Student *t*-test, otherwise with Mann–Whitney test. \* $p < 0.05$ . CIB1, calcium- and integrin-binding protein 1; DAPI, 4',6-diamidino-2-phenylindole.

tested CIB1 over time to understand its expression in both substrates (Figure 2f–h). While endothelial cells in the low-stiffness substrate showed a gradual reduction of CIB1 expression, in the high-stiffness substrate its expression increased over time, as shown in Figure 2b. However, when data were normalized for the compliant substrate, the overall stack from soft to stiff substrate reached a plateau at 24 h.

CIB1 expression was further analyzed at the protein and transcriptional level at 24 and 72 h (Figure 3a,b). Although stiffness upregulated CIB1 after 72 h, data from immunofluorescence in Figure 2g,h suggested that single-cell analysis showed a certain discrepancy between stiff and compliant substrate. Therefore, we planned to analyze HUVECs at low and high confluency, revealing that CIB1 expression is lower when cells adapt to stiff substrate in high confluency but remains higher than in soft conditions (Figure 3c). Further qualitative analysis of cell distribution revealed that polyacrylamide (PAA) gels present a heterogeneous population of cells at low and high confluency (Figure 3d). Our data confirm that cell-to-cell contact increases the complexity level of the ECM-cell coupling mechanism (Ladoux et al., 2016), due to the redistribution of forces, as reviewed elsewhere (Ladoux & Mège, 2017).

### 2.3 | Stiffness modulates CIB1 expression in healthy and cirrhotic LSECs

The effect of matrix stiffness was further evaluated in healthy and cirrhotic rat LSECs. Freshly isolated healthy LSECs showed marked increased CIB1 in response to high stiffness (Figure 4a). To confirm that CIB1 expression was dependent on cellular tension, we inhibited actin and microtubule polymerization by treating healthy LSECs cultured at 30 kPa with cytoskeleton disruption (CD), demonstrating that reduced intracellular tension attenuated the overexpression of CIB1 (Figure 4b). Finally, we evaluated whether reducing intracellular tension by culturing cells on a soft matrix stiffness (0.5 kPa) could reverse CIB1 overexpression in cirrhotic rat LSECs. Interestingly, we found that CIB1 was downregulated in this setting (Figure 4c).

### 2.4 | Stiffness modulates CIB1 translocation in endothelial cells

Recent data demonstrated a proportional relationship between rates of passive diffusion across the nuclear membrane and substrate

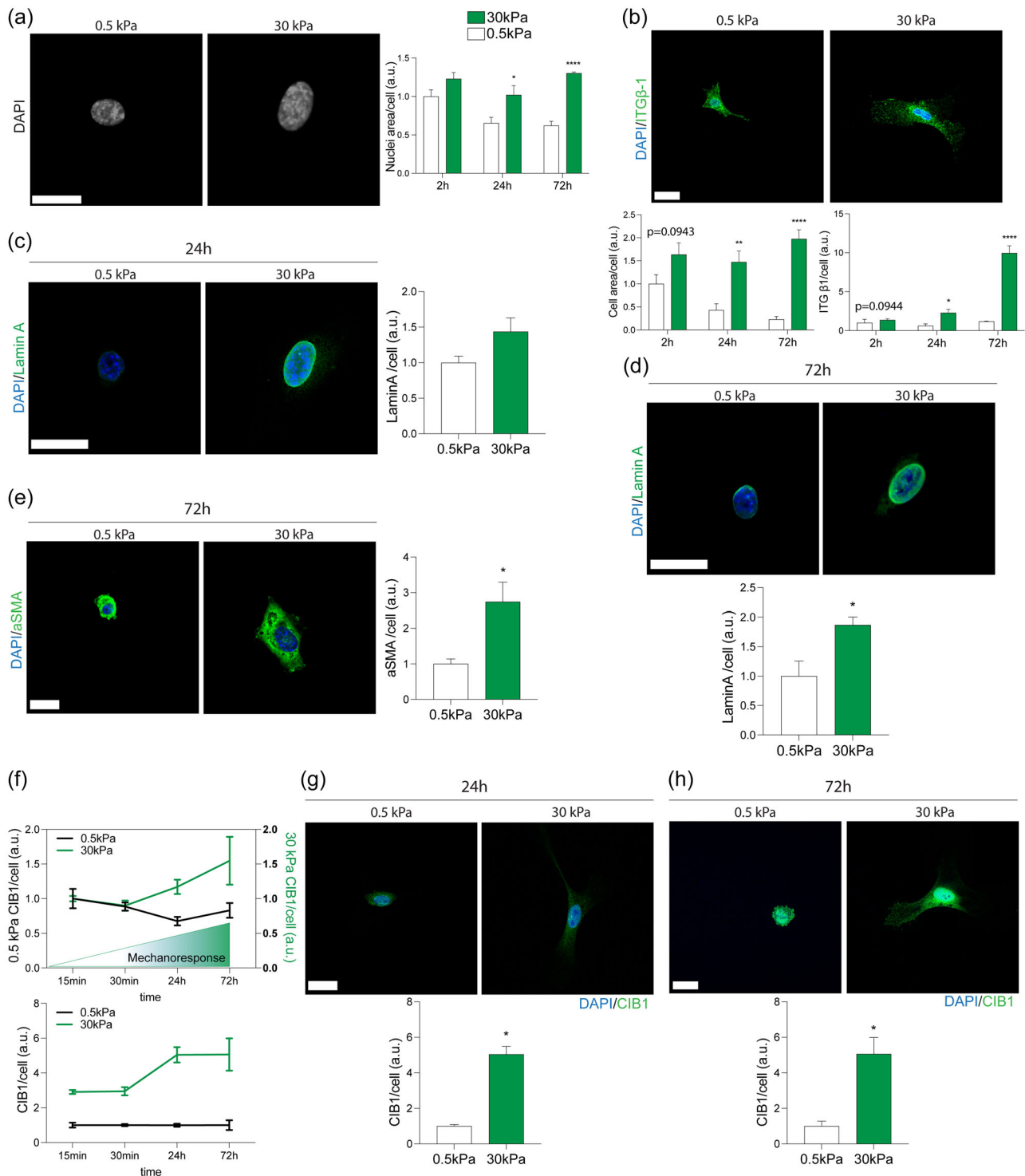


**FIGURE 2** Stiffness modulates CIB1 expression in human endothelial cells. (a, b) Nuclear area (shown by immunofluorescence of DAPI in blue [a]) and cell adhesion and stretching (shown by immunofluorescence of ITG  $\beta$ -1, in green [b]) in HUVECs cultured for 2, 24, and 72 h. Images selected represent the staining of DAPI and ITG  $\beta$ -1 at 72 h. Control group selected for the multiple comparison is 0.5 kPa at every timepoint. (c, d) Immunofluorescence of Lamin A (green) and DAPI (blue) in HUVECs cultured for 24 and 72 h. (e–h) Immunofluorescence of CIB1 (green) in HUVECs cultured at different timepoints. 0.5 and 30 kPa groups were normalized for 15 min timepoint respectively. All scale bars = 20  $\mu$ m. Data derive from at least 50 cells per experimental condition from three to four independent experiments. All ICC data were normalized with the number of cells. For each experiment, sample distributions were assessed for normality (Kolmogorov–Smirnov test). Normally distributed data were compared with unpaired Student *t*-test otherwise with Mann–Whitney test. Data for statistical analysis in time-tests were normalized for 2 h 0.5 kPa and analyzed with two-way ANOVA, Šidák's multiple comparisons test. \**p* < 0.05; \*\**p*  $\leq$  0.01; \*\*\*\**p* < 0.0001, *p* > 0.1 if not specified. CIB1, calcium- and integrin-binding protein 1; DAPI, 4',6-diamidino-2-phenylindole; HUVECs, human umbilical vein endothelial cells; ITG  $\beta$ -1, integrin beta 1;  $\alpha$ SMA, alpha smooth muscle actin.

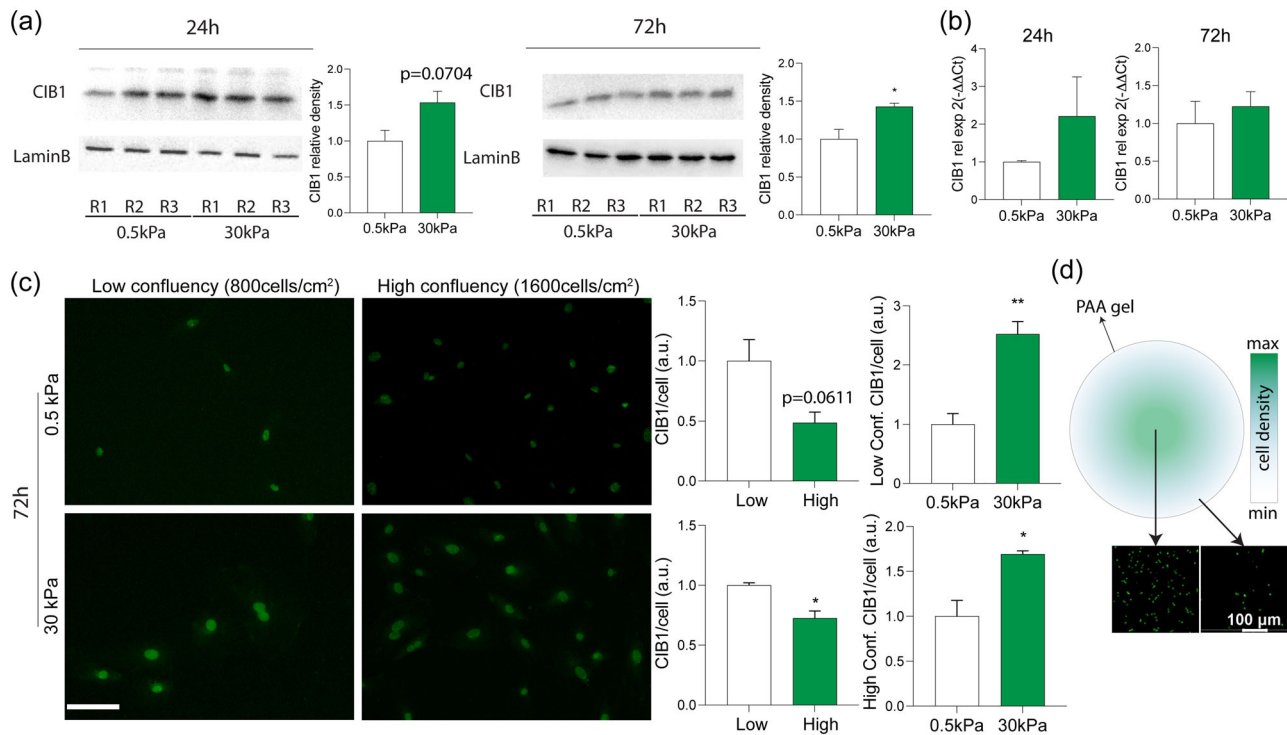


**FIGURE 3** Cell to cell contact influences CIB1 expression. (a) Representative western blots analysis with corresponding quantification of CIB1 (normalized to Lamin B1 expression as housekeeping) in HUVECs cultured for 24 and 72 h. (b) mRNA expression of CIB1 in HUVECs cultured as described in (a). Data were normalized with 18S CT. (c) Immunofluorescence of CIB1 (green) with quantification in HUVECs cultured at low confluency (800 cells/cm<sup>2</sup>) and high confluency (1600 cells/cm<sup>2</sup>) for 72 h. Scale bar = 100  $\mu$ m. Data derived from three independent experiments.  $N > 40$  cells analyzed. Data were normalized for low confluency and 0.5 kPa, respectively. (d) Schematic diagram of gradient cell density from center to periphery and representative image of CIB1 expression. All data derive from  $n = 3$  independent experiments and are expressed as mean  $\pm$  SEM. For each experiment, sample distributions were assessed for normality (Kolmogorov–Smirnov test). Normally distributed data were compared with unpaired Student t-test, otherwise with Mann–Whitney test.  $**p \leq 0.01$ ;  $*p < 0.05$ ,  $p > 0.1$  if not specified. CIB1, calcium- and integrin-binding protein 1; HUVECs, human umbilical vein endothelial cells; PAA, polyacrylamide gels.

stiffness for low molecular weight proteins (Andreu et al., 2022). We thus attempted to understand the kinetics of CIB1 (21 kDa) in response to stiffness. HUVECs or freshly isolated rat LSECs were cultured on 0.5 versus 30 kPa PAA gels for 24 h and intracellular CIB1 fluorescence intensity was quantified. Intriguingly, the cytoplasmic fraction of CIB1 displayed a significant increase on 30 kPa both in HUVECs and in LSECs. The cytoplasmic/nuclear (C/N) ratio was significantly increased in both cell types on high stiffness, pointing toward a mechanically induced net accumulation of CIB1 in the cytoplasm with increasing intracellular tension (Figure 5a,b). To understand if CIB1 translocation was determined by the cellular stiffness and consequent intracellular calcium influx, we reduced the cytoskeletal tension treating LSECs with CD in the 30 kPa PAA. Under these conditions, CIB1 C/N ratio decreased, confirming that the net influx/efflux rates can be reversed by reducing intracellular tension only (Figure 5c). Next, we sought to understand CIB1 dynamics in cirrhotic LSECs, which are characterized by an increased cytoskeletal tension. Freshly isolated cirrhotic LSECs seeded on soft PAA gels displayed decreased cytoplasmic and decreased C/N CIB1 ratio (Figure 5d). Furthermore, we studied the functional localization of CIB1 in healthy and cirrhotic LSECs cultured in their respective

native stiffness, confirming that CIB1 is significantly increased in cirrhotic LSECs cytoplasm (Figure 5e). Finally, we quantified CIB1 fluorescence intensity based on localization in healthy (soft) versus cirrhotic (stiff) human liver LSECs and observed the same pattern as in rat LSECs, with a higher CIB1 concentration in the cytoplasm and increased C/N CIB1 ratio (Figure 5f).

## 2.5 | CIB1 knockdown reduces intracellular tension, improving LSECs phenotype

We next aimed to understand the effects of maintaining low levels of CIB1 under high stiffness conditions in LSECs phenotype. As shown in Figure 6a–c, healthy LSECs cultured at high stiffness with low CIB1 expression exhibited significantly reduced cell and nuclear area, reversing cell stretching and morphology. RNA sequencing revealed 803 differentially expressed genes (DEGs) ( $p < 0.05$ ) when compared to high CIB1 cells. The majority of DEGs were downregulated (78.3%) while 21.6% were upregulated (Figure 6d). By comparing our CIB1 knockdown data set with other three gene sets related with LSECs differentiation revealed that CIB1 downregulation could improve

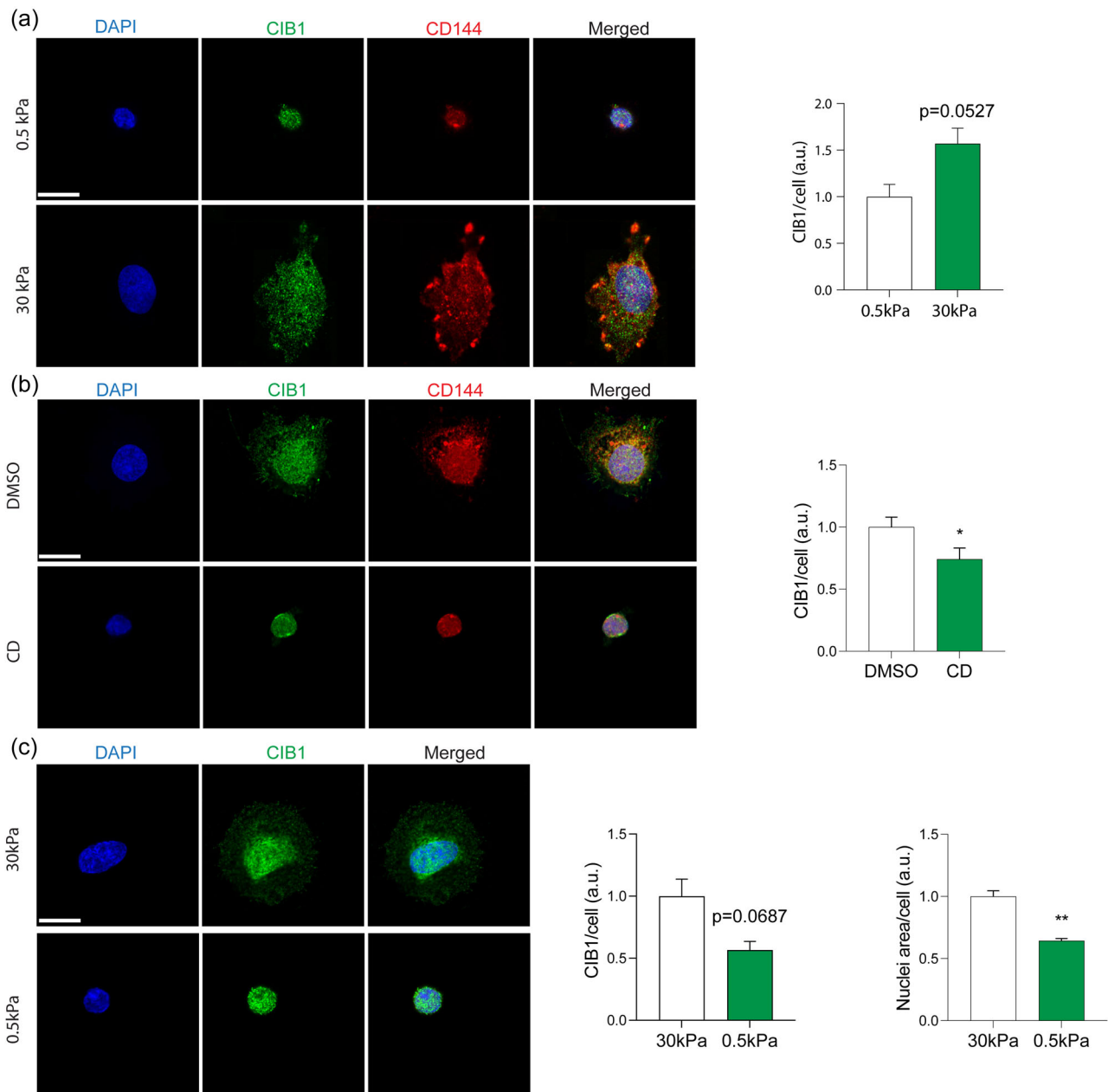


**FIGURE 4** Stiffness modulates CIB1 expression in healthy and cirrhotic LSECs. Immunofluorescence of healthy and cirrhotic rat LSECs, DAPI (blue), CIB1 (green), CD144 (red). (a) LSECs isolated from healthy rats cultured for 24 h in PAA gels at different stiffness ( $n = 269$  in 0.5 kPa and  $n = 219$  in 30 kPa cells from  $n = 5$  independent experiments were analyzed). (b) LSECs isolated from healthy rats cultured in 30 kPa PAA gels and treated for 24 h with CD (2  $\mu$ M cytochalasin D+1  $\mu$ M nocodazole) or DMSO ( $n = 198$  in CD and  $n = 217$  in DMSO cells from  $n = 3$  independent experiments). (c) LSECs isolated from cirrhotic rats cultured for 24 h in PAA gels at different stiffness ( $n = 94$  in 0.5 kPa and  $n = 112$  in 30 kPa cells from three independent experiments). Scale bar 10  $\mu$ m. Data were normalized with the number of cells and are expressed as mean  $\pm$  SEM. For each experiment, sample distributions were assessed for normality (Kolmogorov–Smirnov test). Normally distributed data were compared with unpaired Student *t*-test, otherwise with Mann–Whitney test. \* $p < 0.05$ ; \*\* $p \leq 0.01$ ;  $p > 0.1$  if not specified. CD, cytoskeleton disruption; CIB1, calcium- and integrin-binding protein 1; DAPI, 4',6-diamidino-2-phenylindole; DMSO, dimethyl sulfoxide; LSECs, liver sinusoidal endothelial cells.

LSECs dedifferentiation caused by stiff environment (Figure 6e). Gene set enrichment analysis (GSEA) using gene sets derived by single-cell transcriptomic of healthy liver human cellular niche (Aizarani et al., 2019) revealed a substantial enrichment in siRNA CIB1-treated LSECs. Moreover, GSEA revealed downregulation of

cytoskeleton actin-related gene sets and an upregulation of microtubule-related gene sets, in agreement with a previous report (Naik & Naik, 2011) (Figure 7a,b). Kyoto encyclopedia of genes and genomes (KEGG) analysis revealed downregulation of several pathways involved in mechanosensing such as RHO-GTPase

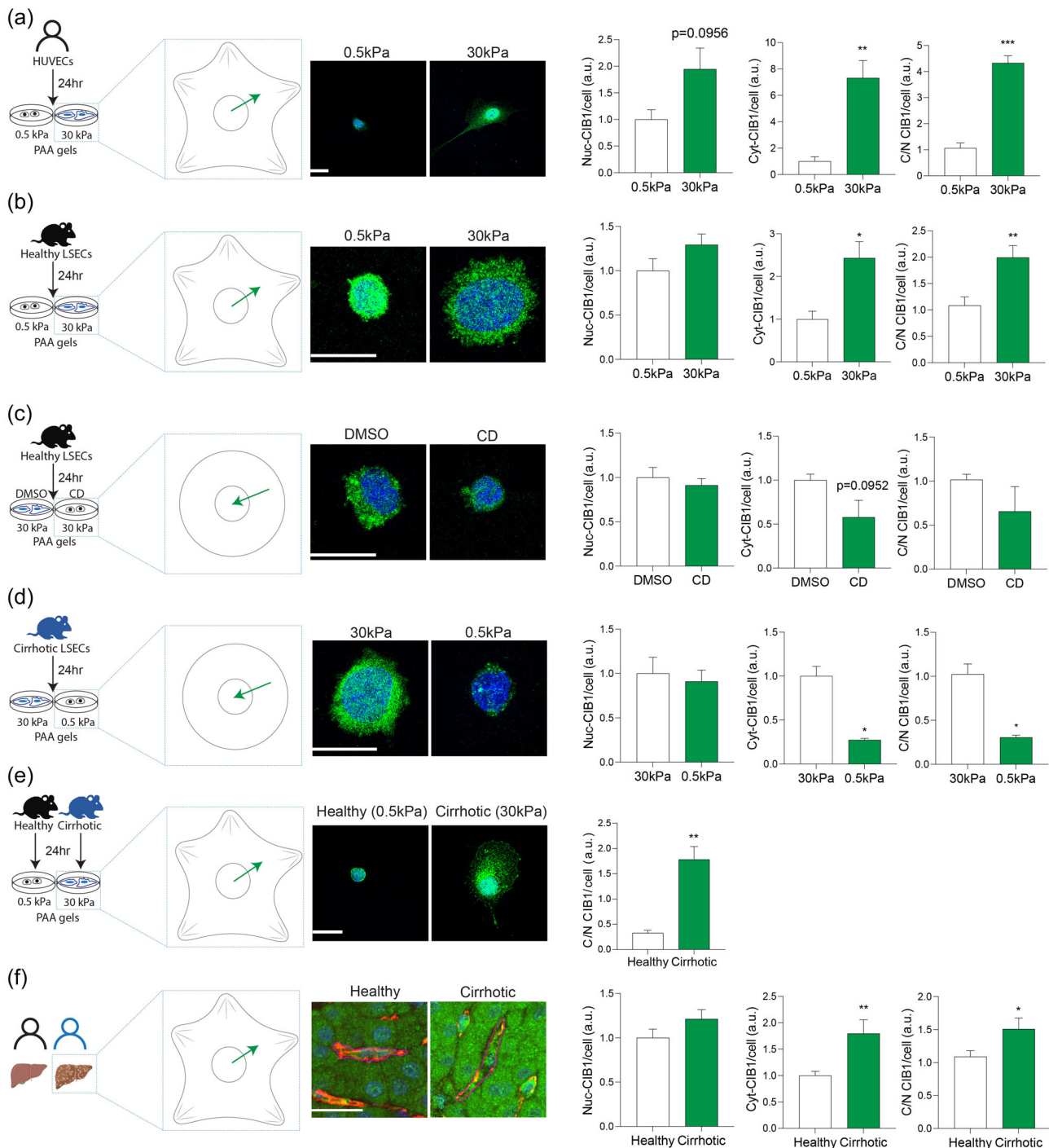


**FIGURE 5** Stiffness modulates CIB1 localization in healthy and cirrhotic endothelial cells. Immunofluorescence in HUVECs, rat LSECs and human liver tissue, DAPI (blue), CIB1 (green), CD144 (red). The arrows indicate the functional accumulation and localization of CIB1, considering the nucleus and cytoplasm as the primary subcellular compartments. (a) HUVEC cultured for 24 h in PAA gels at different stiffness (at least  $n = 40$  cells per condition and replica were analyzed). (b) LSECs isolated from healthy rats cultured for 24 h in PAA gels at different stiffness (at least  $n = 40$  cells per condition and replica were analyzed). (c) LSECs isolated from healthy rats cultured in 30 kPa PAA gels and treated for 24 h with CD ( $2 \mu\text{M}$  cytochalasin D+ $1 \mu\text{M}$  nocodazole) or DMSO ( $n = 269$  in CD and  $n = 219$  in DMSO cells analyzed). (d) LSECs isolated from cirrhotic rats cultured for 24 h in PAA gels at different stiffness ( $n = 94$  in 0.5 kPa and  $n = 112$  in 30 kPa cells analyzed). (e) LSECs isolated from healthy and cirrhotic rats cultured for 24 h in PAA gels in their native stiffness (0.5 kPa-healthy and 30 kPa-cirrhotic; at least  $n = 40$  cells per condition and replica were analyzed). (f) Liver tissue obtained from healthy ( $n = 10$ ) or cirrhotic ( $n = 10$ ) patients (at least  $n = 20$  LSECs analyzed/patient). Scale bar 10  $\mu\text{m}$  for all the figures. Cell data derive from  $n = 3$  to 5 independent experiments. Data were normalized with the number of cells and are expressed as mean  $\pm$  SEM. For each experiment, sample distributions were assessed for normality (Kolmogorov-Smirnov test). Normally distributed data were compared with unpaired Student  $t$ -test otherwise with Mann-Whitney test. \* $p < 0.05$ ; \*\* $p \leq 0.01$ ; \*\*\* $p \leq 0.001$ ;  $p > 0.1$  if not specified. CD, cytoskeleton disruptor; CIB1, calcium- and integrin-binding protein 1; DAPI, 4',6-diamidino-2-phenylindole; DMSO, dimethyl sulfoxide; HUVECs, human umbilical vein endothelial cells; LSECs, liver sinusoidal endothelial cells; PAA, polyacrylamide gels.

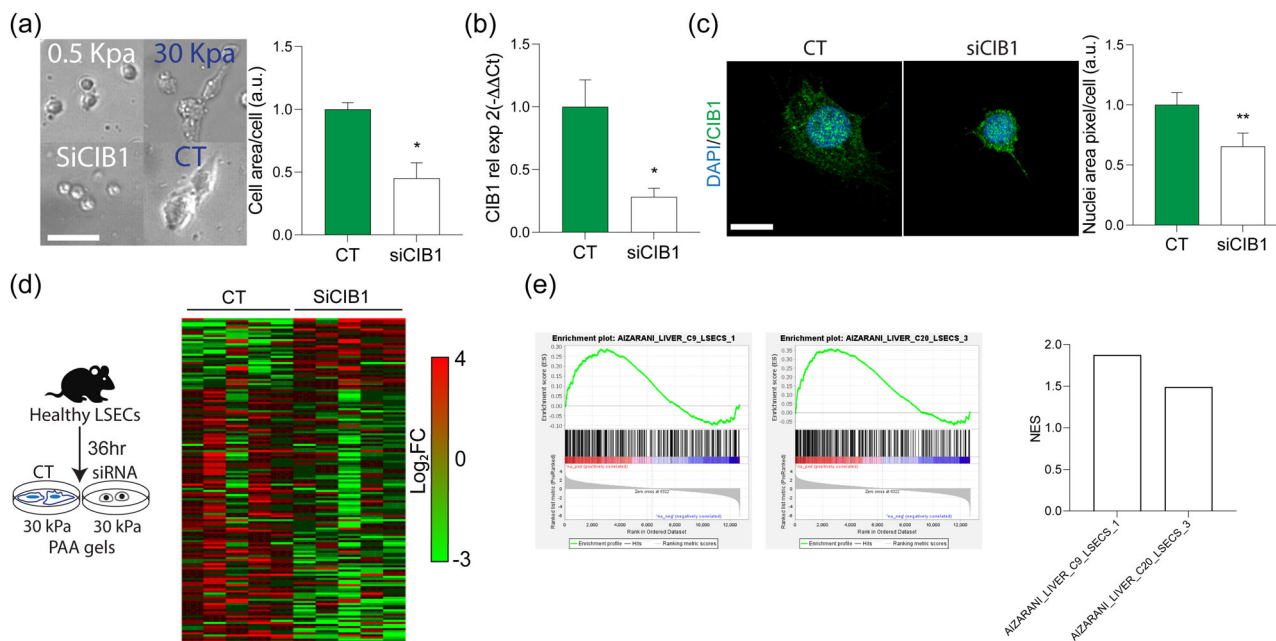


**FIGURE 6** CIB1 knockdown improves LSECs phenotype. (a) Representative images of cell morphology with relative quantification of cell area. Scale bar 125  $\mu\text{m}$ . (b) Knockdown by siRNA of CIB1 in healthy rat LSECs cultured in 30 kPa PAA gels for 36 h. Data derived from five independent experiments. (c) Immunofluorescence of CIB1 (green) and DAPI (blue) of siRNA and control group. Scale bar 10  $\mu\text{m}$ . (d) Heatmap of prefiltered data  $-2 < \text{FC} < 2$  of RNA-seq from healthy rat LSECs treated with siRNA-CIB1 or NT at 30 kPa. (e) GSEA analysis of CIB1 knockdown transcriptomic on two gene sets related with LSECs differentiation revealed that two gene sets were positively correlated (AIRZANI\_Liver\_Cluster9\_LSEC. 1 with NES = 1.8744 and FDR < 0.0001; AIRZANI\_Liver\_Cluster20\_LSEC. 3 with NES = 1.4905 and FDR < 0.0001). (f) Complete list of gene from the leading-edge analysis from GSEA. All the data are expressed as mean  $\pm$  SEM. For each experiment, sample distributions were assessed for normality (Kolmogorov–Smirnov test). Normally distributed data were compared with unpaired Student *t*-test otherwise with Mann–Whitney test. \* $p < 0.05$ ; \*\* $p \leq 0.01$ ;  $p > 0.1$  if not specified. CIB1, calcium- and integrin-binding protein 1; CT, negative control; GSEA, gene set enrichment analysis; LSECs, liver sinusoidal endothelial cells; PAA, polyacrylamide gels; siRNA, small interfering RNA.

(NES =  $-1.7287$ , FDR < 0.05, please find full list in Supporting Information S1: Table 3). From the hallmarks list of GSEA (full list available in Supporting Information S1: Table 4), we observed that downregulated hallmarks were related to allograft rejection, immune response, oxidative stress, and proteins over-represented on the apical surface (Figure 7c). Functional classification of pathways showed that the inflammation mediated by chemokines and cytokine signaling pathway (P00031) was the most represented (Figure 7d). Among the cytokines modulated by CIB1, we found a novel chemokine involved in LSECs dysfunction, C-C motif chemokine 22 (CCL22), that was present in the “allograft rejection” gene set and also involved in the “inflammatory response” gene set. CCL22 downregulation was validated as shown in Figure 7e. Analysis of mRNA expression of CCL22 in healthy LSECs cultured for 24 h at 0.5 and 30 kPa PAA gels revealed that stiffness modulates this cytokine (Figure 7f). Interestingly, we found allograft rejection as the first predicted KEGG pathway with ARCS4 involved with CIB1 expression ( $z\text{-score} = 3.1129$ ; please find full list of pathways in Supporting Information S1: Table 5). Finally, we found that CIB1 expression is mostly involved in biological processes related with actin and microtubule remodeling (full list available in Supporting Information S1: Table 6).

Finally, to assess to what extent CIB1 knockdown can modify gene sets upregulated in CLD, we performed GSEA using publicly available mouse cirrhotic LSECs gene sets obtained from single cell transcriptomic experiments (Su et al., 2021) and observed an inverse correlation between CIB1 knockdown and cirrhotic-specific gene sets (NES =  $-1.96$ , FDR < 0.01) (Figure 8b). Moreover, we generated gene sets based on our human cirrhotic LSECs transcriptomics data set, using the top 100 most upregulated genes in cirrhotic LSECs. GSEA analysis of the expression of cirrhosis-specific genes in the CIB1 knockdown data set showed a decreased enrichment of upregulated genes (NES =  $-2.4$ , FDR < 0.01), thus demonstrating the beneficial effects of CIB1 inhibition on endothelial phenotype (Figure 8c).

### 3 | DISCUSSION

CIB1 is an ubiquitous protein characterized by conformational changes due to  $\text{Ca}^{2+}$  binding, which enables it to interact with other target proteins, thus exerting key cellular functions which may potentially modify cell phenotype (Leisner et al., 2005; Naik & Naik, 2011). Moreover, given its low molecular weight, CIB1 may present increased in/efflux nucleus-cytoplasm rate in response to cell



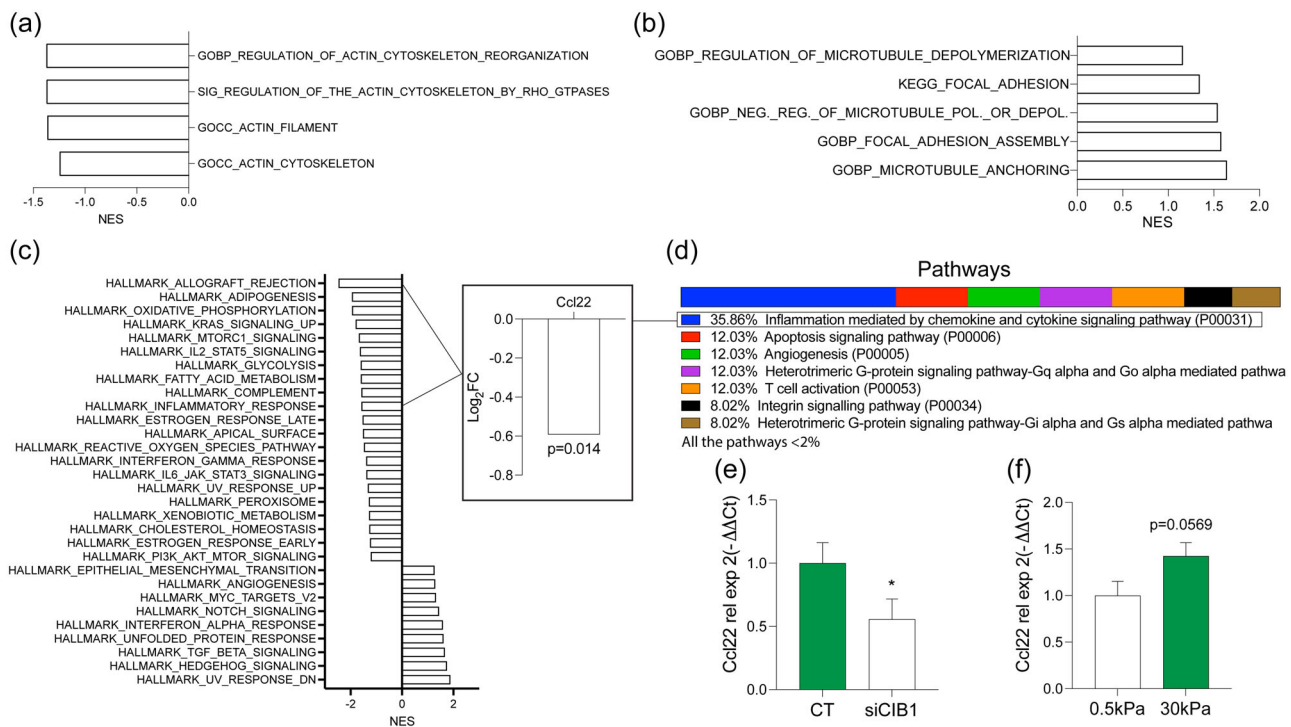


**FIGURE 7** CIB1 knockdown reduces internal stiffness. (a, b) Gene sets relative to cytoskeleton and focal adhesion pathways. (c) RNA-seq Hallmarks from GSEA FDR < 0.1. (d) Functional classification of pathways and molecular function with Panther. Results from classification were filtered for “unclassified” category and the percentage recalculated only on the available classification. (e) mRNA expression of CCL22 in healthy LSECs treated with siRNA-CIB1 and normalized to siRNA-CT. (f) mRNA expression of CCL22 in healthy LSECs cultured in PAA gels with different stiffness (0.5 and 30 kPa) for 24 h. Data derived from six independent experiments. All the data are expressed as mean  $\pm$  SEM. For each experiment, sample distributions were assessed for normality (Kolmogorov–Smirnov test). Normally distributed data were compared with unpaired Student *t*-test otherwise with Mann–Whitney test. \**p* < 0.05; *p*  $\leq$  0.01; *p* > 0.1 if not specified. CCL22, C-C motif chemokine 22; CIB1, calcium- and integrin-binding protein 1; CT, negative control; FC, fold change; GOBP, gene ontology biological process; GOCC, gene ontology cellular component; GSEA, gene set enrichment analysis; LSECs, liver sinusoidal endothelial cells; NES, normalized enrichment score; PAA, polyacrylamide gels; siRNA, small interfering RNA.

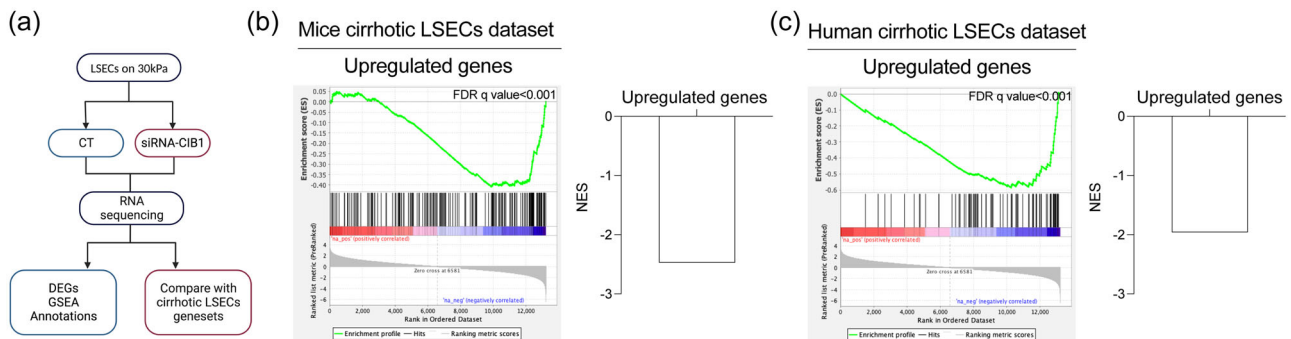


**FIGURE 8** CIB1 knockdown improves LSEC phenotype. (a) Scheme of GSEA analysis workflow. (b) GSEA of the cirrhotic LSEC-specific upregulated gene sets from cirrhotic mouse model were downregulated in the CIB1 knockdown data set. (c) GSEA of the cirrhotic human LSEC-specific upregulated gene sets where downregulated in the CIB1 knockdown data set. CIB1, calcium- and integrin-binding protein 1; CT, negative control; DEGs, differentially expressed genes; GSEA, gene set enrichment analysis; LSECs, liver sinusoidal endothelial cells; siRNA, small interfering RNA.

tension (Andreu et al., 2022). Considering the above, we evaluated the possible role of CIB1 as mechanosensing factor responsible for maintaining the intracellular tension and phenotype dedifferentiation of LSECs under high stiffness, as it happens in advanced CLD.

In this study, we confirmed the increased liver endothelial CIB1 in human cirrhosis, validating previous transcriptomic results (Manicardi et al., 2021) and suggesting its involvement in the progression of advanced CLD, which features increased stiffness

and LSECs dysfunction (Guixé-Muntet et al., 2020; Juin et al., 2013). We also observed CIB1 upregulation along with increased ITG $\beta$ 1 levels under high stiffness conditions (Freeman et al., 2013), suggesting reciprocal influence between CIB1 and integrins, although it may not represent the only mechanism of the effects of CIB1 in mechanotransduction. Indeed, our findings support that cell-to-cell contact influences CIB1 expression in a stiffness-dependent manner. Single LSECs immunofluorescence confirmed how cell-to-cell interactions likely played a role in determining cell tension and reducing CIB1 expression. We further confirmed how cell-to-cell contact affects CIB1 expression in non-hepatic endothelial cells, altogether confirming previous studies on collective versus single cell stretching (Stroka & Aranda-Espinoza, 2011). Moreover, our study found evidence that cell mechanical memory do affect endothelial cells (Rashid et al., 2023; Yang et al., 2014). HUVECs, expanded in plastic, needed longer time to adapt to 0.5 kPa than to 30 kPa, indicating a time-dependent adaptation process. This aligns with CIB1 expression, downregulated in a soft substrate and consistently higher on 30 kPa, a cellular mechanoresponse that was inhibited by abrogating nucleus-cell tensions.

The dynamics of CIB1 levels upon exposure of LSECs to substrates with different stiffness reinforced the observation that this protein has a key role in mechanotransduction. Indeed, normalization of CIB1 levels in LSECs on high stiffness substrate using specific siRNA uncovered its role in mechanotransduction and cell function. GO pathway analysis revealed significant regulation of cytoskeleton-related pathways upon CIB1 knockdown. The interplay between actin and microtubules is crucial for intracellular tension regulation. Indeed, microtubules regulate actin polymerization and myosin contractility, while actin prevent buckling of microtubules (Danowski, 1989; Krendel et al., 2002). Microtubules play a role in suppressing actin bending fluctuations, enabling composite structures to stiffen and relax stress at a slower rate. Actin, on the other hand, supports microtubules against buckling by forming a flexible mesh that permeates the larger microtubule network and absorbs stress to some extent (Ricketts et al., 2018). Overexpressing CIB1 alters actin polymerization and disrupt microtubule organization (Naik & Naik, 2011), while CIB1-depleted cells lack an organized actin cytoskeleton by regulating PAK1 (Leisner et al., 2005). Overall, our findings suggest that CIB1 mediates crosstalk between the actin and microtubule cytoskeletal systems, influencing LSECs phenotype by modulating intracellular tension through actin and microtubule de/polymerization.

GSEA analysis showed functional implications of CIB1 knockdown in LSECs, including dysregulated hallmarks related to inflammation and metabolism. Significant downregulation of mTORC1 upon CIB1 knockdown was observed. Inhibition of mTORC1 suppresses eNOS gene expression due to impaired p70S6K-mediated regulation of KLF2 expression (Wang et al., 2022). In contrast to mTORC1 inhibition, a positive-feedback between MAPK (p38 and JNK) activation and NOX2 upregulation contributes to the excessive generation of reactive oxygen species, which causes eNOS uncoupling and further decrease NO bioavailability in mTORC2-inhibited EC (Wang et al., 2022). Downregulated pathways upon CIB1 knockdown related with cell inflammation included allograft

rejection, complement response, and inflammatory response, suggesting that CIB1 may be involved in inflammation through IL2-STAT5 and IL6-JAK-STAT3. Indeed, mechanical stretch increases chemokine release from LSECs via integrin-dependent activation of transcription factors regulated by Notch and Piezo calcium channel (Hilscher et al., 2019). CIB1 knockdown reduces intracellular tension-derived stress, leading to the downregulation of inflammatory response, including the expression of CCL22. Interestingly, this cytokine interacts with CC chemokine receptor 4 (CCR4), which is the receptor of CCL22 and CCL17 (Scheu et al., 2017) in fibroblasts and endothelial cells (Flytlie et al., 2010; Wang et al., 2023). CCR4 activation triggers TGF- $\beta$ /Smad signaling pathway, contributing to tissue fibrosis (Wang et al., 2023). Although previous studies have reported upregulation of chemokines and cytokines in liver cirrhosis, this is the first time to our knowledge that a CIB1-dependent stiffness-induced modulation of CCL22 is observed in LSECs. This may imply that CIB1-dependent modulation of CCL22 in LSECs can reverse altered LSEC-HSC crosstalk, reducing inflammatory response and attenuating fibrogenesis. Recent studies have involved another cytokine of this class, CCL11 in regulating liver fibrosis by interacting with CCR3 in hepatic stellate cells. Altogether, our observation suggest that mechanical forces may interact with other mechanisms enhancing liver fibrosis (Kong et al., 2023). However, further dedicated studies are requested to clarify CIB1's role in LSECs-HSCs crosstalk in CLD.

Finally, we analyzed the possible role of CIB1 in LSECs redifferentiation. In our study, GSEA analysis versus healthy LSEC gene sets suggests that CIB1 knockdown induces stiffness-related redifferentiation. Moreover, the comparison of CIB1 knockdown LSECs transcriptome with cirrhotic LSEC gene sets (Manicardi et al., 2021; Su et al., 2021) further supported reversal of the dysfunctional phenotype by CIB1 suppression.

We acknowledge some limitations of our study that would merit attention in future research, including the lack of in vivo modulation of CIB1. As CIB1 is a ubiquitous protein involved in many crucial cellular functions, CIB1 targeting would have to be LSECs-selective. Moreover, the effect of CIB1 knockdown on LSECs-HSC cross-talk and promotion of fibrogenesis deserves attention in further studies, given the previously described CCL22-CCR4 axis, which may also play an important role in CLD.

## 4 | MATERIALS AND METHODS

All material and methods are detailed in the Supporting Information Materials section.

### 4.1 | Animals and induction of liver cirrhosis

Female and male Sprague-Dawley rats were purchased and housed in standard environment conditions, with a 12 h/12 h light cycle and 72–77 air exchanges in the animal facility of university Bern. All the

rats were acclimated for 2 weeks upon arrival before starting the experiments and treatments. Rats were provided with a chow diet at libitum and free access to water. All experiments were approved by the Bern Cantonal Ethic Committee and the Laboratory Animal Care (BE892021). To generate a model of cirrhosis with associated PH, thioacetamide (TAA) (Sigma-Aldrich; Ref. No.172502) was administered twice a week at 200 mg/kg of rat body weight (100 mg/mL TAA dissolved in saline) for 12 weeks. Before each administration, body weight was measured, and the dose administered was adjusted accordingly (Boyer-Diaz et al., 2021).

## 4.2 | Human samples

Human tissues were obtained from 20 patients at Inselspital in Switzerland. Ten of these samples were selected from explanted livers from patients with cirrhosis who underwent orthotopic liver transplantation. Ten samples of non-cirrhotic liver were obtained from patients with similar age and gender who underwent partial hepatectomy for liver metastasis or hepatic echinococcosis resection. All samples and associated clinical information were collected with informed consent of patients and all the experiments were approved by Ethics Committee (KEK 2021-01403).

## 4.3 | Isolation of liver endothelial sinusoidal cells

Isolation of primary cells was performed as previously described (Fernández-Iglesias et al., 2019). Please see the Supporting Information Materials for further details regarding cell isolation and pharmacological treatments.

## 4.4 | Preparation of PAA with different stiffness

PAA coated with collagen were prepared as previously described (Guixé-Muntet et al., 2020) and detailed in the Supporting Information Materials section. Gels' stiffness was established at 0.5 and 30 kPa (Young's modulus), respectively to mimic the environment of healthy and cirrhotic-like shear modulus, as previously published (Berzigotti, 2017; Levental et al., 2007).

## 4.5 | Cell culture

Freshly isolated LSECs were grown in Dulbecco's Modified Eagle's Medium/Nutrient Mixture F-12 (Gibco; 11330032) with 10% fetal bovine serum (Gibco; A4766801), 1% antibiotic-antimycotic (Sigma; A5955), 50 µg/mL endothelial cell growth supplement (ECGS) (Merck; 02-102), and 100 µg/mL heparin (Sigma; H-3393). HUVECs were purchased from Lonza and cultured in Medium 199 (Sigma-Aldrich; M4530) with 20% fetal bovine serum, 1% antibiotic-antimycotic, 50 µg/mL ECGS, and 100 µg/mL heparin. Cells were incubated at 37°C in a humid atmosphere

with 5% CO<sub>2</sub>. Regarding CD experiment in healthy LSECs, cells were treated with a combination of 2 µM cytochalasin D (Sigma; C2618) plus 1 µM nocodazole (Sigma; M1404) or vehicle (dimethylsulfoxide; Sigma; 41647) for 24 h.

## 4.6 | CIB1 mRNA silencing and transcriptomic analysis

To further investigate the CIB1 function in mechanotransduction, predesigned small interfering RNA (siRNA) for CIB1 and negative control (CT) siRNA were purchased from Thermo Fisher Scientific (s135830, s135829, 4390846). Freshly isolated LSECs plated on 3 kPa PAA gels for 12 h were transfected with validated CIB1 siRNA and NT siRNA at a final concentration of 10 nM in the presence of Lipofectamine RNAiMAX (Thermo Fisher Scientific; 13778030). 7.5 µL Lipofectamine RNAiMAX was mixed with 117.5 µL OptiMEM and incubated 10 min at RT. CIB1 siRNA and negative control siRNA were diluted to 10 nM with OptiMEM in a volume of 125 µL. Incubate these two mixes for 10 min at RT. Meanwhile, LSEC were washed with warm PBS and OptiMEM. Finally, each well was filled with 1750 µL OptiMEM and transfection mixture 250 µL and incubated for 6 h. After 6 h, 1000 µL media contained 30% FBS, 150 µg/mL ECGS; then 300 µg/mL heparin was added to each well. Cells were harvested after another 24 h for continued analysis. Please see detailed information about RNA-seq in Supporting Information Materials.

## 4.7 | Real-time quantitative PCR

Real-time PCR was performed using TaqMan probes. Analysis of the transcriptome of LSECs was performed at the Next Generation Sequencing platform of the University of Bern. Please see detailed information in Supporting Information Materials.

## 4.8 | Immunofluorescence and microscopy

Cells for immunohistochemistry were fixed directly on the PAA gels with 4% paraformaldehyde for 10 min, rinsed with PBS, and permeabilized with 0.1% triton X-100 (Sigma) for 5 min. Unspecific binding was blocked with 1% bovine serum albumin for 30 min. Cells were incubated with primary antibody against CIB1 (1:200, Proteintech #11823-1-AP; 1:200, Thermo Fisher Scientific #PA5-83931) and CD144 (1:200, Thermo Fisher Scientific #14-1449-82) to mark the endothelial cells membrane at 4°C overnight. Secondary antibody incubation was performed with Goat Anti-Rabbit IgG H&L Alexa Fluor® 488 (1:500; Abcam #ab150077) and Goat Anti-Mouse IgG H&L Cy5® (1:1000; Abcam #ab6563) in combination with 4',6-diamidino-2-phenylindole (DAPI) for 1 h at room temperature. Slides were then mounted with fluorescent aqueous mounting medium (Dako; S302380-2) and dried overnight. Please see Supporting

Information Materials section for details about processing of the samples, imaging, and quantification of molecular targets.

#### 4.9 | Bioinformatic analysis

A pre-expansion of gene network was made with Enrichr via ARCHS<sup>4</sup> RNA-seq gene-gene coexpression matrix to identify the genes that mostly c-express with CIB1. Enrichr (<https://maayanlab.cloud/Enrichr/>) is a web-portal developed by the Ma'ayan lab at the Data Coordination and Integration Center at Icahn School of Medicine at Mount Sinai (Chen et al., 2013; Kuleshov et al., 2016). Network expansion was made by selecting Reactome database including the top 10 genes related with the pre-expanded list (<https://maayanlab.cloud/enrichr-kg>). Prediction of CIB1 related pathways and biological process was performed with (ARCHS<sup>4</sup>) (<https://maayanlab.cloud/archs4/>) (Lachmann et al., 2018) which is a resource that provides access to gene and transcript counts uniformly processed from all human and mouse RNA-seq experiments from the Gene Expression Omnibus and the Sequence Read Archive.

#### 4.10 | Statistical analysis

Statistical analyses were performed using GraphPad Prism 6 (GraphPad Software). Data represent biological replicates ( $n$ ) and were depicted as mean values  $\pm$  standard error (SEM). Frequency distribution of data was assessed with Normality test (Kolmogorov–Smirnov). For samples characterized by a normal distribution, means were compared by the Student  $t$ -test (two samples) or ANOVA ( $>2$  samples) followed by the Tukey post hoc analysis. Nonparametric tests (Kruskal–Wallis) followed by Mann–Whitney  $U$  test were used otherwise. Difference was considered significant at  $p < 0.05$ .

#### AUTHOR CONTRIBUTIONS

Cong Wang, Eric Felli, and Sonia Selicean designed the research, performed the experiments, analyzed the data, and wrote the paper. Yelidusi Nulan performed experiments. Juan José Lozano analyzed the data. Sergi Guixé-Muntet and Jaume Bosch conceived ideas and critically revised the paper. Annalisa Berzigotti conceived ideas, obtained funding, and critically revised the paper. Jordi Gracia-Sancho conceived the study, designed and directed the research, obtained funding, and wrote the paper. All authors edited and reviewed the final version of the manuscript.

#### ACKNOWLEDGMENTS

This study was carried out at the Department for Biomedical Research at the University of Bern and at the Esther Koplowitz Center, Institut d'Investigacions Biomèdiques August Pi i Sunyer (IDIBAPS) in Barcelona. Funders of this study had no role in study design, data collection and analysis, decision to publish, or preparation of the paper. The authors are indebted to Philipp Kellmann and Carlos Wotzkow for technical support. The authors acknowledge the Translational Research

Unit at the Institute of Pathology, University of Bern, Switzerland, for excellent technical support and Tissue Bank Bern for providing the human tissue samples. This project was supported by the Swiss National Science Foundation (SNF 320030\_189252/1), the Novartis Foundation, the Swiss Foundation against Liver Cancer, the Instituto de Salud Carlos III (FIS PI20/00220, PI23/00945, and DTS22/00010, cofunded by the European Union), and the AGAUR-Generalitat de Catalunya (2021 SGR 01322 & 2021 PROD 00036). CIBEREHD is funded by the Instituto de Salud Carlos III. Part of the work was funded by own research funds of the Hepatology group, Department of Visceral Surgery and Medicine, Inselspital, Bern. C. W. is supported by the China Scholarship Council (CSC), and by the Stiftung für Leberkrankheiten, Bern. S. S. is supported by the Juan Rodés Fellowship from the European Association for the Study of the Liver and the Swiss Government Excellence Scholarships, and by the Stiftung für Leberkrankheiten, Bern. S. G.-M. is supported by a Sara Borrell Fellowship from Instituto de Salud Carlos III. Open access funding provided by Inselspital Universitätsspital Bern.

#### CONFLICT OF INTEREST STATEMENT

J. B. is a consultant for Astra-Zeneca, BioVie, Boehringer-Ingelheim, Novo-Nordisk, and Resolution Therapeutics. A. B. is a consultant for Boehringer-Ingelheim. The remaining authors declare no conflict of interest.

#### ORCID

Jordi Gracia-Sancho  <http://orcid.org/0000-0001-7736-4089>

#### REFERENCES

- Aizarani, N., Saviano, A., Sagar, M., Maily, L., Durand, S., Herman, J. S., Pessaux, P., Baumert, T. F., & Grün, D. (2019). A human liver cell Atlas reveals heterogeneity and epithelial progenitors. *Nature*, 572(7768), 199–204. <https://doi.org/10.1038/s41586-019-1373-2>
- Andreu, I., Granero-Moya, I., Chahare, N. R., Klein, K., Molina-Jordán, M., Beedle, A. E. M., Elosegui-Artola, A., Abenza, J. F., Rossetti, L., Trepast, X., Raveh, B., & Roca-Cusachs, P. (2022). Mechanical force application to the nucleus regulates nucleocytoplasmic transport. *Nature Cell Biology*, 24(6), 896–905. <https://doi.org/10.1038/s41556-022-00927-7>
- Armacki, M., Joodi, G., Nimmagadda, S. C., de Kimpe, L., Pusapati, G. V., Vandoninck, S., Van Lint, J., Illing, A., & Seufferlein, T. (2014). A novel splice variant of calcium and integrin-binding protein 1 mediates protein kinase D2-stimulated tumour growth by regulating angiogenesis. *Oncogene*, 33(9), 1167–1180. <https://doi.org/10.1038/ncr.2013.43>
- Berzigotti, A. (2017). Non-invasive evaluation of portal hypertension using ultrasound elastography. *Journal of Hepatology*, 67(2), 399–411. <https://doi.org/10.1016/j.jhep.2017.02.003>
- Berzigotti, A., Seijo, S., Arena, U., Abralde, J. G., Vizzutti, F., García-Pagán, J. C., Pinzani, M., & Bosch, J. (2013). Elastography, spleen size, and platelet count identify portal hypertension in patients with compensated cirrhosis. *Gastroenterology*, 144(1), 102–111. <https://doi.org/10.1053/j.gastro.2012.10.001>
- Boyer-Diaz, Z., Aristu-Zabalza, P., Andrés-Rozas, M., Robert, C., Ortega-Ribera, M., Fernández-Iglesias, A., Broqua, P., Junien, J. L., Wettstein, G., Bosch, J., & Gracia-Sancho, J. (2021). Pan-PPAR agonist lanifibranor improves portal hypertension and hepatic fibrosis in experimental advanced chronic liver disease. *Journal of*

- Hepatology*, 74(5), 1188–1199. <https://doi.org/10.1016/j.jhep.2020.11.045>
- Chen, E. Y., Tan, C. M., Kou, Y., Duan, Q., Wang, Z., Meirelles, G. V., Clark, N. R., & Ma'ayan, A. (2013). Enrichr: Interactive and collaborative HTML5 gene list enrichment analysis tool. *BMC Bioinformatics*, 14, 128. <https://doi.org/10.1186/1471-2105-14-128>
- Cooper, J., & Giancotti, F. G. (2019). Integrin signaling in cancer: Mechanotransduction, stemness, epithelial plasticity, and therapeutic resistance. *Cancer Cell*, 35(3), 347–367. <https://doi.org/10.1016/j.ccell.2019.01.007>
- Danowski, B. A. (1989). Fibroblast contractility and actin organization are stimulated by microtubule inhibitors. *Journal of Cell Science*, 93(Pt 2), 255–266. <https://doi.org/10.1242/jcs.93.2.255>
- Fernández-Iglesias, A., Ortega-Ribera, M., Guixé-Muntet, S., & Gracia-Sancho, J. (2019). 4 in 1: Antibody-free protocol for isolating the main hepatic cells from healthy and cirrhotic single rat livers. *Journal of Cellular and Molecular Medicine*, 23(2), 877–886. <https://doi.org/10.1111/jcmm.13988>
- Fletcher, D. A., & Mullins, R. D. (2010). Cell mechanics and the cytoskeleton. *Nature*, 463(7280), 485–492. <https://doi.org/10.1038/nature08908>
- Flytlie, H. A., Hvid, M., Lindgreen, E., Kofod-Olsen, E., Petersen, E. L., Jørgensen, A., Deleuran, M., Vestergaard, C., & Deleuran, B. (2010). Expression of MDC/CCL22 and its receptor CCR4 in rheumatoid arthritis, psoriatic arthritis and osteoarthritis. *Cytokine*, 49(1), 24–29. <https://doi.org/10.1016/j.cyto.2009.10.005>
- Freeman, Jr., T. C., Black, J. L., Bray, H. G., Dagliyan, O., Wu, Y. I., Tripathy, A., Dokholyan, N. K., Leisner, T. M., & Parise, L. V. (2013). Identification of novel integrin binding partners for calcium and integrin binding protein 1 (CIB1): Structural and thermodynamic basis of CIB1 promiscuity. *Biochemistry*, 52(40), 7082–7090. <https://doi.org/10.1021/bi400678y>
- Gracia-Sancho, J., Caparrós, E., Fernández-Iglesias, A., & Francés, R. (2021). Role of liver sinusoidal endothelial cells in liver diseases. *Nature Reviews Gastroenterology & Hepatology*, 18(6), 411–431. <https://doi.org/10.1038/s41575-020-00411-3>
- Gracia-Sancho, J., Marrone, G., & Fernández-Iglesias, A. (2019). Hepatic microcirculation and mechanisms of portal hypertension. *Nature Reviews Gastroenterology & Hepatology*, 16(4), 221–234. <https://doi.org/10.1038/s41575-018-0097-3>
- Greuter, T., Yaqoob, U., Gan, C., Jalan-Sakrikar, N., Kostallari, E., Lu, J., Gao, J., Sun, L., Liu, M., Sehrawat, T. S., Ibrahim, S. H., Furuta, K., Nozickova, K., Huang, B. Q., Gao, B., Simons, M., Cao, S., & Shah, V. H. (2022). Mechanotransduction-induced glycolysis epigenetically regulates a CXCL1-dominant angiocrine signaling program in liver sinusoidal endothelial cells in vitro and in vivo. *Journal of Hepatology*, 77(3), 723–734. <https://doi.org/10.1016/j.jhep.2022.03.029>
- Grund, A., Szaroszyk, M., Döppner, J. K., Malek Mohammadi, M., Kattih, B., Korf-Klingebiel, M., Gigina, A., Scherr, M., Kensah, G., Jara-Avaca, M., Gruh, I., Martin, U., Wollert, K. C., Gohla, A., Katus, H. A., Müller, O. J., Bauersachs, J., & Heineke, J. (2019). A gene therapeutic approach to inhibit calcium and integrin binding protein 1 ameliorates maladaptive remodelling in pressure overload. *Cardiovascular Research*, 115(1), 71–82. <https://doi.org/10.1093/cvr/cvy154>
- Guixé-Muntet, S., Ortega-Ribera, M., Wang, C., Selicean, S., Andreu, I., Kechagia, J. Z., Fondevila, C., Roca-Cusachs, P., Dufour, J. F., Bosch, J., Berzigotti, A., & Gracia-Sancho, J. (2020). Nuclear deformation mediates liver cell mechanosensing in cirrhosis. *JHEP Reports*, 2(5), 100145. <https://doi.org/10.1016/j.jhep.2020.100145>
- Hilscher, M. B., Sehrawat, T., Arab, J. P., Zeng, Z., Gao, J., Liu, M., Kostallari, E., Gao, Y., Simonetto, D. A., Yaqoob, U., Cao, S., Revzin, A., Beyder, A., Wang, R. A., Kamath, P. S., Kubes, P., & Shah, V. H. (2019). Mechanical stretch increases expression of CXCL1 in liver sinusoidal endothelial cells to recruit neutrophils, generate sinusoidal microthrombi, and promote portal hypertension. *Gastroenterology*, 157(1), 193–209. <https://doi.org/10.1053/j.gastro.2019.03.013>
- Juin, A., Planus, E., Guillemot, F., Horakova, P., Albiges-Rizo, C., Génot, E., Rosenbaum, J., Moreau, V., & Saltel, F. (2013). Extracellular matrix rigidity controls podosome induction in microvascular endothelial cells. *Biology of the Cell*, 105(1), 46–57. <https://doi.org/10.1111/boc.201200037>
- Kalukula, Y., Stephens, A. D., Lammerding, J., & Gabriele, S. (2022). Mechanics and functional consequences of nuclear deformations. *Nature Reviews Molecular Cell Biology*, 23(9), 583–602. <https://doi.org/10.1038/s41580-022-00480-z>
- Kanchanawong, P., & Calderwood, D. A. (2022). Organization, dynamics and mechanoregulation of integrin-mediated cell-ECM adhesions. *Nature Reviews Molecular Cell Biology*, 24(2), 142–161. <https://doi.org/10.1038/s41580-022-00531-5>
- Killaars, A. R., Grim, J. C., Walker, C. J., Hushka, E. A., Brown, T. E., & Anseth, K. S. (2019). Extended exposure to stiff microenvironments leads to persistent chromatin remodeling in human mesenchymal stem cells. *Advanced Science*, 6(3), 1801483. <https://doi.org/10.1002/adv.201801483>
- Kong, M., Dong, W., Kang, A., Kuai, Y., Xu, T., Fan, Z., Shi, L., Sun, D., Lu, Y., Li, Z., & Xu, Y. (2023). Regulatory role and translational potential of CCL11 in liver fibrosis. *Hepatology*, 78(1), 120–135. <https://doi.org/10.1097/HEP.0000000000000287>
- Krendel, M., Zenke, F. T., & Bokoch, G. M. (2002). Nucleotide exchange factor GEF-H1 mediates cross-talk between microtubules and the actin cytoskeleton. *Nature Cell Biology*, 4(4), 294–301. <https://doi.org/10.1038/ncb773>
- Kuleshov, M. V., Jones, M. R., Rouillard, A. D., Fernandez, N. F., Duan, Q., Wang, Z., Koplev, S., Jenkins, S. L., Jagodnik, K. M., Lachmann, A., McDermott, M. G., Monteiro, C. D., Gundersen, G. W., & Ma'ayan, A. (2016). Enrichr: A comprehensive gene set enrichment analysis web server 2016 update. *Nucleic Acids Research*, 44(W1), W90–W97. <https://doi.org/10.1093/nar/gkw377>
- Lachmann, A., Torre, D., Keenan, A. B., Jagodnik, K. M., Lee, H. J., Wang, L., Silverstein, M. C., & Ma'ayan, A. (2018). Massive mining of publicly available RNA-seq data from human and mouse. *Nature Communications*, 9(1), 1366. <https://doi.org/10.1038/s41467-018-03751-6>
- Ladoux, B., & Mège, R. M. (2017). Mechanobiology of collective cell behaviours. *Nature Reviews Molecular Cell Biology*, 18(12), 743–757. <https://doi.org/10.1038/nrm.2017.98>
- Ladoux, B., Mège, R. M., & Treppe, X. (2016). Front-rear polarization by mechanical cues: From single cells to tissues. *Trends in Cell Biology*, 26(6), 420–433. <https://doi.org/10.1016/j.tcb.2016.02.002>
- Leisner, T. M., Freeman, T. C., Black, J. L., & Parise, L. V. (2016). CIB1: A small protein with big ambitions. *The FASEB Journal*, 30(8), 2640–2650. <https://doi.org/10.1096/fj.201500073R>
- Leisner, T. M., Liu, M., Jaffer, Z. M., Chernoff, J., & Parise, L. V. (2005). Essential role of CIB1 in regulating PAK1 activation and cell migration. *The Journal of Cell Biology*, 170(3), 465–476. <https://doi.org/10.1083/jcb.200502090>
- Levental, I., Georges, P. C., & Janmey, P. A. (2007). Soft biological materials and their impact on cell function. *Soft Matter*, 3(3), 299–306. <https://doi.org/10.1039/b610522j>
- Manicardi, N., Fernández-Iglesias, A., Abad-Jordà, L., Royo, F., Azkargorta, M., Ortega-Ribera, M., Sanfeliu-Redondo, D., Martínez-Alcocer, A., Elortza, F., Hessheimer, A. J., Fondevila, C., Lozano, J. J., García-Pagán, J. C., Bosch, J., Cubero, F. J., Albillos, A., Vaquero, J., Falcón-Pérez, J. M., & Gracia-Sancho, J. (2021). Transcriptomic profiling of the liver sinusoidal endothelium during cirrhosis reveals stage-specific secretory signature. *Cancers*, 13(11), 2688. <https://www.mdpi.com/2072-6694/13/11/2688>

- Martin, K., Pritchett, J., Llewellyn, J., Mullan, A. F., Athwal, V. S., Dobie, R., Harvey, E., Zeef, L., Farrow, S., Streuli, C., Henderson, N. C., Friedman, S. L., Hanley, N. A., & Piper Hanley, K. (2016). PAK proteins and YAP-1 signalling downstream of integrin beta-1 in myofibroblasts promote liver fibrosis. *Nature Communications*, 7, 12502. <https://doi.org/10.1038/ncomms12502>
- Miroshnikova, Y. A., Manet, S., Li, X., Wickström, S. A., Faurobert, E., & Albiges-Rizo, C. (2021). Calcium signaling mediates a biphasic mechanoadaptive response of endothelial cells to cyclic mechanical stretch. *Molecular Biology of the Cell*, 32(18), 1724–1736. <https://doi.org/10.1091/mbc.E21-03-0106>
- Naik, M. U., & Naik, U. P. (2011). Calcium- and integrin-binding protein 1 regulates microtubule organization and centrosome segregation through polo like kinase 3 during cell cycle progression. *The International Journal of Biochemistry & Cell Biology*, 43(1), 120–129. <https://doi.org/10.1016/j.biocel.2010.10.003>
- Nasrollahi, S., Walter, C., Loza, A. J., Schimizzi, G. V., Longmore, G. D., & Pathak, A. (2017). Past matrix stiffness primes epithelial cells and regulates their future collective migration through a mechanical memory. *Biomaterials*, 146, 146–155. <https://doi.org/10.1016/j.biomaterials.2017.09.012>
- Parsons, J. T., Horwitz, A. R., & Schwartz, M. A. (2010). Cell adhesion: Integrating cytoskeletal dynamics and cellular tension. *Nature Reviews Molecular Cell Biology*, 11(9), 633–643. <https://doi.org/10.1038/nrm2957>
- Rashid, F., Liu, W., Wang, Q., Ji, B., Irudayaraj, J., & Wang, N. (2023). Mechanomemory in protein diffusivity of chromatin and nucleoplasm after force cessation. *Proceedings of the National Academy of Sciences*, 120(13), e2221432120. <https://doi.org/10.1073/pnas.2221432120>
- Ricketts, S. N., Ross, J. L., & Robertson-Anderson, R. M. (2018). Co-entangled actin-microtubule composites exhibit tunable stiffness and power-law stress relaxation. *Biophysical Journal*, 115(6), 1055–1067. <https://doi.org/10.1016/j.bpj.2018.08.010>
- Rosales, O. R., Isales, C. M., Barrett, P. Q., Brophy, C., & Sumpio, B. E. (1997). Exposure of endothelial cells to cyclic strain induces elevations of cytosolic Ca<sup>2+</sup> concentration through mobilization of intracellular and extracellular pools. *Biochemical Journal*, 326(Pt 2), 385–392. <https://doi.org/10.1042/bj3260385>
- Scheu, S., Ali, S., Ruland, C., Arolt, V., & Alferink, J. (2017). The C-C chemokines CCL17 and CCL22 and their receptor CCR4 in CNS autoimmunity. *International Journal of Molecular Sciences*, 18(11), 2306. <https://doi.org/10.3390/ijms18112306>
- Slack, R. J., Macdonald, S. J. F., Roper, J. A., Jenkins, R. G., & Hatley, R. J. D. (2022). Emerging therapeutic opportunities for integrin inhibitors. *Nature Reviews Drug Discovery*, 21(1), 60–78. <https://doi.org/10.1038/s41573-021-00284-4>
- Stroka, K. M., & Aranda-Espinoza, H. (2011). Effects of morphology vs. cell-cell interactions on endothelial cell stiffness. *Cellular and Molecular Bioengineering*, 4(1), 9–27. <https://doi.org/10.1007/s12195-010-0142-y>
- Su, T., Yang, Y., Lai, S., Jeong, J., Jung, Y., McConnell, M., Utsumi, T., & Iwakiri, Y. (2021). Single-cell transcriptomics reveals zone-specific alterations of liver sinusoidal endothelial cells in cirrhosis. *Cellular and Molecular Gastroenterology and Hepatology*, 11(4), 1139–1161. <https://doi.org/10.1016/j.jcmgh.2020.12.007>
- Trebicka, J., Gu, W., de Ledinghen, V., Aubé, C., Krag, A., Praktikno, M., Castera, L., Dumortier, J., Bauer, D. J. M., Friedrich-Rust, M., Pol, S., Grgurevic, I., Zheng, R., Francque, S., Gottfriedová, H., Mustapic, S., Sporea, I., Berzigotti, A., Uschner, F. E., ... Jansen, C. (2022). Two-dimensional shear wave elastography predicts survival in advanced chronic liver disease. *Gut*, 71(2), 402–414. <https://doi.org/10.1136/gutjnl-2020-323419>
- Walker, C. J., Crocini, C., Ramirez, D., Killaars, A. R., Grim, J. C., Aguado, B. A., Clark, K., Allen, M. A., Dowell, R. D., Leinwand, L. A., & Anseth, K. S. (2021). Nuclear mechanosensing drives chromatin remodelling in persistently activated fibroblasts. *Nature Biomedical Engineering*, 5(12), 1485–1499. <https://doi.org/10.1038/s41551-021-00709-w>
- Wang, Q., Liu, S., Min, J., Yin, M., Zhang, Y., Zhang, Y., Tang, X., Li, X., & Liu, S. (2023). CCL17 drives fibroblast activation in the progression of pulmonary fibrosis by enhancing the TGF- $\beta$ /Smad signaling. *Biochemical Pharmacology*, 210, 115475. <https://doi.org/10.1016/j.bcp.2023.115475>
- Wang, Y., Li, Q., Zhang, Z., Peng, K., Zhang, D.-M., Yang, Q., Passerini, A. G., Simon, S. I., & Sun, C. (2022). mTOR contributes to endothelium-dependent vasorelaxation by promoting eNOS expression and preventing eNOS uncoupling. *Communications Biology*, 5(1), 726. <https://doi.org/10.1038/s42003-022-03653-w>
- Yang, C., Tibbitt, M. W., Basta, L., & Anseth, K. S. (2014). Mechanical memory and dosing influence stem cell fate. *Nature Materials*, 13(6), 645–652. <https://doi.org/10.1038/nmat3889>
- Zayed, M. A., Yuan, W., Chalothorn, D., Faber, J. E., & Parise, L. V. (2010). Tumor growth and angiogenesis is impaired in CIB1 knockout mice. *Journal of Angiogenesis Research*, 2, 17. <https://doi.org/10.1186/2040-2384-2-17>
- Zayed, M. A., Yuan, W., Leisner, T. M., Chalothorn, D., McFadden, A. W., Schaller, M. D., Hartnett, M. E., Faber, J. E., & Parise, L. V. (2007). CIB1 regulates endothelial cells and ischemia-induced pathological and adaptive angiogenesis. *Circulation Research*, 101(11):1185–1193. <https://doi.org/10.1161/circresaha.107.157586>

## SUPPORTING INFORMATION

Additional supporting information can be found online in the Supporting Information section at the end of this article.

**How to cite this article:** Wang, C., Felli, E., Selicean, S., Nulan, Y., Lozano, J. J., Guixé-Muntet, S., Bosch, J., Berzigotti, A., & Gracia-Sancho, J. (2024). Role of calcium integrin-binding protein 1 in the mechanobiology of the liver endothelium. *Journal of Cellular Physiology*, 1–14. <https://doi.org/10.1002/jcp.31198>